

유리섬유 강화 열가소성 복합재료 판재의 소성가공

이 중 희*

Deep Drawing of Glass Fiber Reinforced Thermoplastic Composite

J. H. Lee*

ABSTRACT

유리섬유가 강화된 열가소성 복합재료 판재의 성형성에 대한 이해를 돕기 위해 이론적 고찰과 실험적 고찰이 행해졌다. 성형 시험에 사용된 형상은 임의의 방향으로 위치한 유리섬유를 중량비로 30% 함유한 폴리프로필렌 재료가 사용되었고, 시험된 형상은 판재의 굽힘성이나 인장성을 측정하는데 널리 사용되는 스위프트컵(Swift flat-bottomed cup)모양이다. 성형시험과 재료 시험은 폴리프로필렌 Matrix의 유리성 천이온도(Glass transition temperature)와 용융온도 사이에서 행해졌다. 본 연구의 이론적 고찰을 위해서 재료의 평면 방향으로는 동질성을 그리고 그 직각 방향으로는 이질성을 가진 연속체 물질로 가정하여 유도하였다. 이러한 이론적 결과는 실험 결과와 비교되어졌고, 이를 통해 시험된 재료의 최적의 성형조건을 제시하였다.

Key Words: Glass Fiber Reinforced Thermoplastic Composite(유리섬유 강화 열가소성 복합재료), Solid-Phase Forming(고상성형), Deep Drawing(딥 드로잉), Formability(성형성)

1. Introduction

Fiber reinforced polymeric composites provide the desirable properties of high strength and stiffness as well as low specific weight. Hence, they have become some of the most important materials in the automotive, aerospace and other industries⁽¹⁻³⁾.

These composites can be grouped into thermoplastic composites and thermoset composites, with thermoplastic composites having several advantages over thermoset composites in mechanical properties and in processing^(4, 5). As a result,

the study of the material behavior and forming techniques of such composites has attracted considerable attention in recent years⁽⁶⁻⁸⁾. One of the most promising of the forming techniques of thermoplastic composites is solid-phase forming. Solid-phase forming is the forming process in which the part is formed at temperatures between their glass transition temperature and melting point. The major advantages of solid-phase forming are very short cycle time and good surface finish⁽⁹⁾.

Since Ito reported the deep drawing of plastics at room temperature and test methods for drawa-

* 전북대학교 기계공학부

bility in the 1950's⁽¹⁰⁾, many studies have been done to investigate the formability of plastics. Several researchers have applied metal working techniques to the solid-phase forming of plastics in cup forming, for example, Broutman and Kalpakjian⁽¹¹⁾, Di Pede and Woodhams⁽¹²⁾, Faz-zari et al.⁽¹³⁾, and Prevorsek et al.⁽¹⁴⁾. War-shavsky and Tokita suggested that the modified cup test was the most reliable for measuring cold drawability of the thermoplastic sheets⁽¹⁵⁾. The theory of deep drawing of metals was also applied to thermoplastics by Evans⁽¹⁶⁾ and Miles and Miles⁽¹⁷⁾. Several finite element analyses to predict the behavior of polycarbonate sheets under simple solid-phase cup forming process were made by Lee and coworkers^(18,19).

The above works were all performed using unreinforced plastic materials. In contrast, solid-phase forming processes for thermoplastic composite materials have received much less attention. There is still a need for more studies about the formability of thermoplastic composite sheets. In most cases, thermoplastic composites processing conditions are established based on experience. A number of test conditions should be done to get a satisfactory result. This is very costly and inefficient. Therefore some research has been done in modeling the forming process of thermoplastic composites. Especially, development of a model for thermoplastic composites is very important in improving process design and operation.

The objective of this research has been to model the forming process of thermoplastic composites and to investigate the formability of a particular composite sheet in solid-phase forming. This analytical work was done to predict strain distributions according to the plane stress theory.

2. Analysis Method

The analytical model described here is based on the axi-symmetrical plane stress characteristic

theory described by Szczepinski⁽²⁰⁾. The basic assumption for plane stress conditions is $\tau_{r\theta} = 0$, with σ_r and σ_θ which are distributed uniformly across the thickness of the sheet. The material used in this analysis is assumed to be incompressible. The yield stress of the material is considered as function of temperature only. For axial symmetry, the equilibrium equation under the plane stress condition can be written as^(20,21):

$$\frac{d}{dr}(\sigma_r r h) - \sigma_\theta h = 0 \quad (1)$$

where h is the thickness of the sheet and r is radius of an element as shown in Fig. 1.

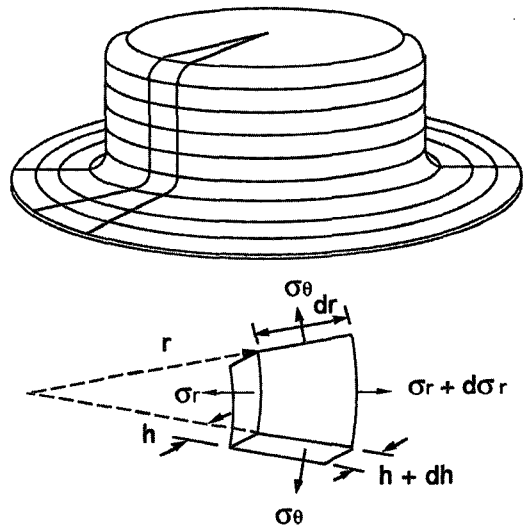


Fig. 1 Descriptions of a force balance element for analysis of axisymmetric cup forming.

The incompressibility condition can be expressed as:

$$d\epsilon_r + d\epsilon_\theta + d\epsilon_h = 0 \quad (2)$$

The strain rate $d\epsilon_r$ and $d\epsilon_\theta$ can be expressed in terms of radial velocity V_r as:

$$d\epsilon_r = \frac{\partial V_r}{\partial r} \quad d\epsilon_\theta = \frac{V_r}{r} \quad (3)$$

The strain rate of thickness deh can be represented by making use of the formula for a thickness increment in an element:

$$dh = \frac{\partial h}{\partial r} dr + \frac{\partial h}{\partial t} dt \quad (4)$$

$$d\varepsilon_h = \frac{1}{h} \left(\frac{\partial h}{\partial t} + V_r \frac{\partial h}{\partial r} \right) \quad (5)$$

With Equations (3) and (5), the incompressibility equation can be represented by

$$\frac{1}{h} \left(\frac{\partial h}{\partial t} + V_r \frac{\partial h}{\partial r} \right) + \frac{\partial V_r}{\partial r} + \frac{V_r}{r} = 0 \quad (6)$$

The Von Mises yield condition, with rotationally symmetric anisotropic yield represented by a single R-value following Hill's theory of anisotropy^(22, 23):

$$\sigma_r^2 - \frac{2R}{1+R} \sigma_r \sigma_\theta + \sigma_\theta^2 = Y^2 \quad (7)$$

where the parameter R represents the ratio of the width to thickness strains in a uniaxial tension test and Y is the yield stress. The flow rule associated with Equation (7) takes the form:

$$\frac{d\varepsilon_r}{\sigma_r - \frac{R}{1+R} \sigma_\theta} = \frac{d\varepsilon_\theta}{\sigma_\theta - \frac{R}{1+R} \sigma_r} \quad (8)$$

There are four equations: the equilibrium equation (1), the incompressibility equation (6), the yield condition (7) and flow rule (8), and four unknowns: σ_r , σ_θ , V_r and h. To solve a set of four equations, the method of characteristic is used. The differential equations of the first family of characteristics are

$$dr = V_r dt = 0 \quad (9)$$

$$\frac{dh}{dr} = \frac{h}{r} \frac{\sigma_r + \sigma_\theta}{R\sigma_r - (1+R)\sigma_\theta} \quad (10)$$

These characteristics describe the path of particular particles in the r, t plane, that is, the stress and deformation history which a particle undergoes. Whereas, the differential equations of second family of characteristics are

$$t = \text{constant} \quad (11)$$

$$\frac{dV_r}{dr} = \frac{V_r}{r} \frac{\sigma_r - \frac{R}{1+R} \sigma_\theta}{\sigma_\theta - \frac{R}{1+R} \sigma_r} \quad (12)$$

These characteristics represent deformations of all the particle at each instant. Fig. 2 describes the cup forming process with the first and second families of characteristics. Along the characteristics of the second family, the following differential equation can be derived from the equilibrium equation as follows:

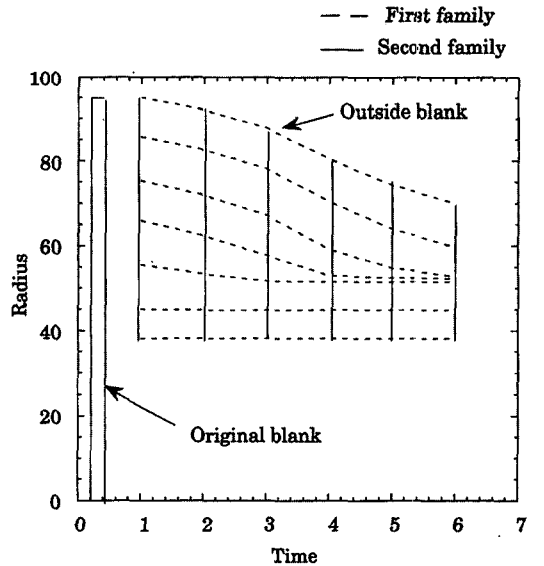


Fig. 2 Descriptions of the first family and second family of characteristics.

$$\frac{dh}{dr} = \frac{h}{r} \frac{\sigma_r - \sigma_\theta}{\sigma_r} - \frac{h}{\sigma_r} \frac{d\sigma_r}{dr} \quad (13)$$

An auxiliary function ω is made such that the Von Mises yield condition is satisfied. Then the stress components σ_r and σ_θ can be expressed

as:

$$\sigma_r = Y \frac{\sqrt{2R+1}}{R+1} \cos(\omega - \phi) \quad (14)$$

$$\sigma_\theta = Y \frac{\sqrt{2R+1}}{R+1} \cos(\omega + \phi) \quad (15)$$

$$\text{where } \phi = \tan^{-1} \frac{1}{\sqrt{2R+1}}$$

Substituting these relations into the differential equations of characteristics, we have the final form of equations for the first family of characteristics:

$$dr - V_r dt = 0 \quad (16)$$

$$\frac{dh}{dr} = \frac{h}{r} \frac{\cos(\omega - \phi) + \cos(\omega + \phi)}{R \cos(\omega - \phi) - (1+R) \cos(\omega + \phi)} \quad (17)$$

For the second family of characteristics, where $t = \text{constant}$, we have

$$\frac{dV_r}{dr} = \frac{V_r}{r} \frac{\cos(\omega + \phi) - \frac{R}{1+R} \cos(\omega - \phi)}{\cos(\omega - \phi) - \frac{R}{1+R} \cos(\omega + \phi)} \quad (18)$$

$$\frac{dh}{dr} = \frac{h}{r} \left(1 - \frac{\cos(\omega + \phi)}{\cos(\omega - \phi)}\right) + h \tan(\omega - \phi) \frac{d\omega}{dr} - \frac{h}{Y} \frac{dY}{dr} \quad (19)$$

In order to solve these ordinary differential equations, it is necessary to find the stress boundary condition and the velocity boundary condition with some additional approximation. One of the basic assumptions of this theory is that the material is rigid-perfect-plastic, but stress is considered as a function of strain rate and temperature. And another assumption is that the radial stress at the end of the blank is zero, that is, $\sigma_r = 0$. Thus along this end line, the value of ω equals to $\pi/2 + \phi$ because the circumferential stress is compressive for the cup forming process. Now to integrate the differential equation, the Equation (19) can be rewritten for $d\omega/dr$ as:

$$\begin{aligned} \frac{d\omega}{dr} = & \frac{1}{\tan(\omega - \phi) Y} \frac{1}{dr} \frac{dY}{dr} + \frac{1}{h \tan(\omega - \phi)} \frac{dh}{dr} \\ & + \frac{1}{r \tan(\omega - \phi)} \left(1 - \frac{\cos(\omega + \phi)}{\cos(\omega - \phi)}\right) \end{aligned} \quad (20)$$

where dY/dr is obtained from the difference of

values of yield stress between neighboring nodes, which can be obtained from the material test under the same conditions of sheet forming (temperature, punch speed). For the first step, thickness is assumed to be uniform at every node. With this initial condition and with the stress boundary condition, in doing the integration of this differential Equation (20), fourth order Runge-Kutta methods are used⁽²²⁾. For the next step integration, the thickness difference dh/dr can be calculated from the Equation (17).

Once the value of ω at each node has been calculated from the Equation (20), the velocity boundary condition is applied at the boundary to integrate the differential Equation (18). Here the velocity condition is based on a geometric calculation of the movement of the material in the punch profile region. Any material initially lying beneath the flat bottom of the punch is assumed to not deform, while material beneath the punch profile region is assumed to wrap without thickness change over the punch profile as the punch moves into the material. The deformation computed is uniform around the circumference, with thickness constancy maintained exactly. Based on the movement of the material in the punch profile regions and taking into account the slope of free section of the sheet which is assumed to be straight between the punch and die, the velocity required to keep the continuity between material in the punch and material outside the punch region is computed. The velocity boundary condition in sheet direction is applied to the point which is computed punch contact point for the next stage. By using the geometric relationship between the velocity in radial direction and the velocity in sheet direction, the integration of the differential Equation (18) is performed.

3. Experimental Investigation

The material used in the this research was 30

% glass fiber reinforced polypropylene composite sheets manufactured by AZDEL. The average glass fiber length and diameter were reported by the manufacturer to be 12.25 mm and 16 μm , respectively, and the glass transition and the melting temperature of the matrix were $-10\text{ }^{\circ}\text{C}$ and $165\text{ }^{\circ}\text{C}$. The thickness of the sheet was 3.18 mm.

The yield strength of the composite was evaluated using tension tests. The tests were performed on an MTS tension test machine with a high temperature chamber to obtain yield stress measurements at different temperatures and strain rates. For each test, the specimen was kept in the chamber for 30 minutes to allow it to reach the desired temperature before testing. The overall tension test procedure followed ASTM D638 as closely as possible. The R-value of each sample was calculated by measuring the thickness strain and transverse strain measured after fracture and cooling. Because no clear relationship was found between strain rate and yield stress over the range from 0.001/sec to 0.01/sec, the effect of strain rate was neglected in this study. Fig. 3 shows how the measured yield stress varied with temperature and strain rate for the material. Points in the figure are the experimental results and lines are interpolated between

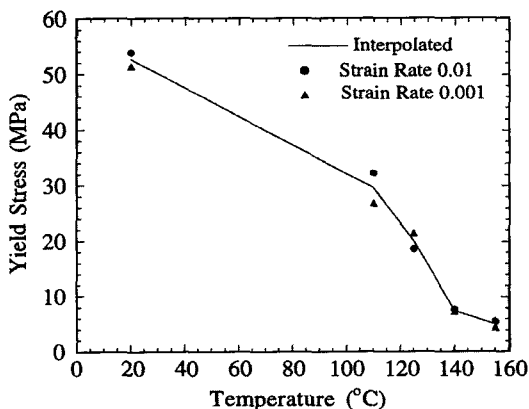


Fig. 3 Measured yield stress for 30 % glass fiber reinforced polypropylene composite.

experimental data. Since no significant trend of R-value with temperatures is observed, the average R-value, that is, $R=0.49$, was used in the analysis.

The cup forming test is one that has been widely used to test the formability of sheet material. This forming process is composed of two main deformation, that is, compressive deformation in the hoop direction and tensile deformation in the radial direction. The formability depends upon lubrication and tooling, as well as on material properties in the sheet. In this study, a number of cups were formed to test the formability of a specific material and to compare with the analytical predictions. Circular cups were formed from circular blanks on a modified double-acting PHI hydraulic press. The experiments were performed at temperatures ranging from $110\text{ }^{\circ}\text{C}$ to $150\text{ }^{\circ}\text{C}$, with the radial temperature gradient in the sheet varied for each setting. The blank geometry and forming parameters used for each cup are summarized in Table 1. The geometry of the punch and die used for these tests is given in Table 2. A sample formed cup at temperature of $135\text{ }^{\circ}\text{C}$ is shown in Fig. 4. To measure the strains in the formed cups, an automated strain measurement system was used^(23,24).

Table 1 Blank size and forming parameters.

Temperature ($^{\circ}\text{C}$)	110, 135, 150
Cup shape	Circular
Blank shape	Circle
Blank size (mm)	184, 190
Punch speed (mm/sec)	0.4
Punch depth (mm)	40, 45

Table 2 Die and punch geometry.

Punch size (mm)	101.6
Die size (mm)	114.3
Clearance (mm)	6.4
Punch profile radius (mm)	12.7
Die profile radius (mm)	12.7

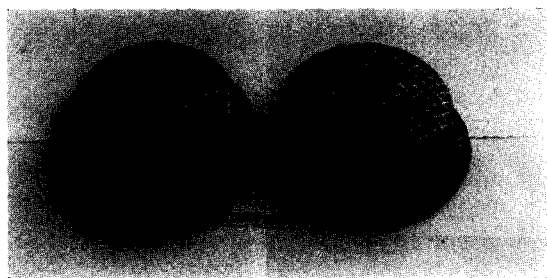


Fig. 4 A sample cup formed at temperature of 135 °C.

4. Comparison and Results

To find the effect of R-value on the strain distribution, the cup strains at various R-values are shown in the Fig. 5. The forming temperature of 150 °C and the punch depth of 40 mm were used in this analysis. When the R-value was increasing, the major strain and minor strain were also increasing.

Although the material was initially assumed to have uniformly distributed fiber orientation in the plane of the sheet, it became clear during testing that the production of the sheet had induced a preferred fiber direction. As a result, both the shape of the formed cup and the measured strain distributions were not symmetric. For the comparison of strains along a radial line, strain-distance figure was plotted. The major and minor

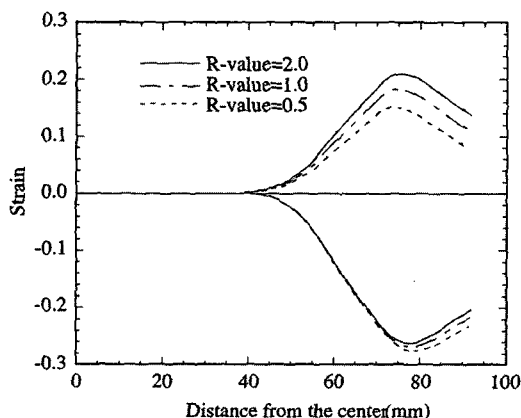


Fig. 5 Predicted strain distributions at various R-values

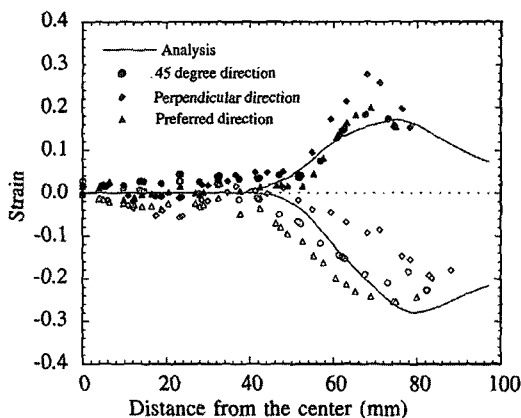


Fig. 6 Comparison of predicted and experimental strains at 100°C along a radial section.

strains obtained from three different radial sections are shown in Fig. 6. Strains in the middle of the thickness along the diagonal of the cup were compared. Qualitative agreement between the average of measured major or minor strains and analysis can be seen.

Wrinkling is an undesirable mode of deformation in deep drawing. It is caused by the compressive hoop stress induced by the drawing force. It is very important to anticipate and predict wrinkling in a forming process because it results in an unacceptable surface appearance and a potentially weakened part. Necking is also undesirable in deep drawing because it weakens the final product. The wrinkling and necking in the formed cup are shown in Fig 7.

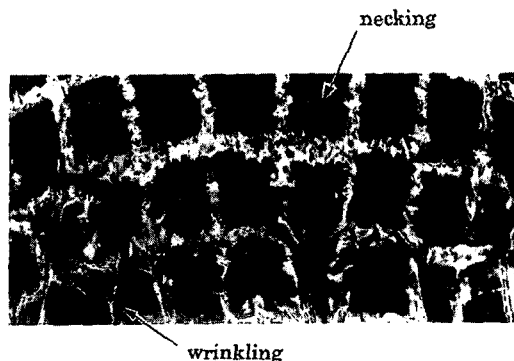


Fig. 7 Wrinkling and necking observed on the formed cup.

5. Conclusion and Recommendation

The plane stress analysis described in this work has been applied to the modeling of glass fiber reinforced polypropylene composite sheet forming. As shown in Fig. 5, this approximate method captures the main trends of the data. However, there is a discrepancy in a defined section with the measurements in the preferred fiber direction and direction perpendicular to the preferred direction which the model is not able to take into account. One of main sources of this error is the fact that the axi-symmetric model can not incorporate the planar anisotropy of the material. Therefore, for better analytical results, a three dimensional model including planar anisotropy should be developed for this composite forming. The high R-value means larger minor strain than that of low R-value when the thickness strain is fixed.

The existence of a preferred fiber direction in this material makes the formed cups unsymmetric in shape which may be undesirable in forming parts. As expected, the forming limit for wrinkling was related to the preferred fiber direction and associated with the R-value. Forming without necking for this tested material was limited to small major strains, typically less than 10 percent.

Better formability was observed for this composite material sheet with a flange region temperature ranging from 130 °C to 150 °C.

References

1. Bigg, D. M. and Preston, J. R. "Stamping of Thermoplastic Matrix Composites" *Polymer Composites* Vol. 10 No. 4 pp 261-268, 1989.
2. Crosby, Jane M. "Recent Advances in Thermoplastic Composites" *Advanced Material and Processes Inc. Metal Progress* pp 56-59, 1988.
3. Fallon, Michael R. "Thermoplastic Sheet Stamping : Ready for the Big Time" *lastic Technology* pp 95-103, 1989.
4. Muzzy, J. D. , Wu, X. and Colton, J. S. "Thermoforming of High Performance Thermoplastic Composites" *ANTEC* pp 1465-1470, 1989.
5. Tennyson, R. C., Waterhouse, T. A., Newman, Takemori, S., M. and Wright, A. N. "Panel Discussion on : Thermoplastics vs Thermosets in Advanced Composites" *Polymer Composites* Vol. 8 No. 6 pp 437-440, 1987.
6. Smiley, A. J. and Pipes, R. B. "Analysis of the Diaphragm Forming of Continuous Fiber Reinforced Thermoplastics" *Journal of Thermoplastic Composite Materials*, Vol. 1, pp 298-321, 1990.
7. Tsahalis, D. T., Pantelakis, S. G. and Schulze, V. "Modeling of the Diaphragm Forming Technique Applied to Continuous Fiber Reinforced Thermoplastic Composites" *Processing of Polymers and Polymeric Composites MD-Vol. 19*, pp 91-101, 1990.
8. Wu, Xiang "Thermoforming continuous Fiber Reinforced Thermoplastic Composites" Ph. D. Thesis, Georgia Institute of Technology, 1990
9. Bigg, D.M., Hiscock, D.F., Preston, J.R., and Bradbury, E.J. "Thermoplastic Matrix Sheet composites" *Polymer Composites* Vol. 9, No. 3, pp 222-228, 1988.
10. Ito, K. "The Plastic Working Ability Test of Sheet Plastics by a Deep Drawing Process" *Proceedings of the Third U.S. National Congress of Applied Mechanics*, pp 563, June, 1958.
11. Broutman, L. J. and Kalpakjian, S. "Cold Forming of Plastics" *SPE Journal*, Vol. 25, pp 46-52, Oct. 1969
12. Di Pede, Sandro and Woodhams, Raymond T. "Deep Drawing Self-Reinforced Thermo-

- plastic Sheet" *Polymer Engineering and Science* Vol. 30 No. 19 pp 1185-1199, 1990.
13. Fazzari, A. M., Hofer, P. H., Backie, R. L., and Luther, C. H. "Stamping of Azdel Reinforced Thermoplastic Sheet" *SPE 30th Annual Technical Conference*, pp 500-506, May, 1972.
 14. Prevorsek, D. C., Koch, P. J., Oswald, H. J., and Li, H. L. "Cold Forming of Plastic Part II. Draw Forming of Laminates Containing Crosslinkable Core" *Polymer Engineering and Science*, Vol. 11 No. 2, pp 109-123, Mar. 1971.
 15. Warskavsky, M. and Tokita, N. "Cold Drawability of Thermoplastic sheets" *SPE Journal*, Vol. 26, pp 55-58, Aug. 1970.
 16. Evans, Robert E. "The Mechanical Behavior of Thermoplastic Materials in Deep Drawing Process" *Polymer Engineering and Science* Vol. 13, No.1, pp 65-73, 1973.
 17. Miles, M. J. and Mills, N. J. "The Deep Drawing of Thermoplastics" *Polymer Engineering and Science* Vol. 17, No. 2, pp 101-110, Feb. 1977.
 18. Lee, D. and Luken, P. C. "Material Modeling and Solid Phase Forming of Polycarbonate Sheet" *Polymer Engineering and Science* Vol. 26, No. 9, pp 612~619, May, 1986.
 19. Lee, D., Amoedo, J., Jung, G., and Vogel, J. H. "Solid-Phase Processing of Thermoplastic Materials" *Proceedings of the 14th Conference on Production Research and Technology*, University of Michigan, Ann Arbor, MI, 1987.
 20. Szczepinski, Wojciech, *Introduction to the Mechanics of Plastic Forming of Metals*, Sijthoff and Noordhoff International Publishers B. V., Alphen aan den Rijn, Netherlands, 1990.
 21. Hill, R., *The Mathematical Theory of Plasticity*, Oxford University Press, London, 1983.
 22. Gerald, Curtis F. and Wheatley, Partrick O., *Applied Numerical Analysis*, Addison-wesley, June, 1989.
 23. Vogel, J. H. and Lee, D., "Computerized Method of Determining Surface Strain Distributions on a Deformed Body" U.S. Patent No. 4969106, 1989.
 24. Vogel, J. H. and Lee, D., "An Analysis Method for Deep Drawing Process Design" *International Journal of Mechanical Sciences*, Vol. 32, pp 891-07, 1990.